Duty cycle-based isolation in linear quadrupole ion traps

Rachit Singh, Vivek Jayaram, Peter T.A. Reilly *

Washington State University, Department of Chemistry, Fulmer 128, Pullman, WA 99164, United States

ARTICLE INFO

ABSTRACT

Simulation and matrix methods were used to determine the change in the minimum trapping frequency during duty cycle base waveform manipulation to provide axial trapping. Duty cycle based axial trapping sets both rod sets of a digitally driven linear quadrupole to the same potential thereby nullifying the radial trapping field for a definable interval during the waveform cycle. Turning off the radial trapping field affects the ion motion. Consequently, the ion stability conditions and the secular frequency change with duty cycle during axial trapping. The work presented here demonstrates the change in the ion motion by simulating the ion trajectories under duty cycle base trapping conditions and determining the change in the minimum trapping frequency as a function of the change in duty cycle. The change in the stability conditions with duty cycle was determined by matrix methods. These calculations were used to determine the minimum trapping frequency change with duty cycle and validate the simulations. They were then used to discuss the duty cycle effects and propose methodology for using duty cycle waveform manipulation to perform precise ion isolation. Finally, matrix methods were used to show that ion isolation can be performed concurrently with duty cycle based axial trapping. These results were confirmed by simulation.

© 2013 Elsevier B.V. All rights reserved.

1. Introduction

Previously, our group simulated duty cycle-based trapping and ejection of massive ions using digitally driven linear quadrupole traps [1]. More recently, we showed that this technology was a key element in the well-resolved mass analysis of singly charged intact proteins out to 205 kDa (intact myosin) and beyond [2]. The presented technology traps ions of any size [3] at the end of a linear quadrupole ion trap where they are translationally cooled by buffer gas collisions and then ejects them in a well-collimated plug with narrowly definable kinetic energy into an awaiting orthogonal acceleration time-of-flight mass analyzer (oa-TOF-MS). The ability to manipulate the duty cycles of the trapping waveforms permits control of the ion trajectories into oa-TOF-MS that provides resolved mass analysis of the entire range of intact singly charged proteins.

Obtaining significantly higher resolution in the ultra high mass range ($m/z > 20,000$) is only one benefit of duty cycle-based waveform manipulation technology. To take full advantage of our trapping technology, ion isolation using duty cycle manipulated waveforms would be beneficial. This has already been accomplished in a digitally driven linear quadrupole by operating it as a mass filter [4,5]. In this mode, the duty cycle of one applied

quadrupole waveform (E_1) is shifted from the typical value of 50% (50% high and 50% low). The other waveform (E_2) is created by inverting the waveform on E1. These waveforms have been illustrated in Fig. 1(a). As drawn, the time averaged potential on electrode set E1 has net negative value while the time averaged potential on E_2 has a net positive value. The time averaged potential difference between the rods sets ($\overline{E_1} - \overline{E_2}$) creates the DC potential necessary to operate the quadrupole as a mass filter. Changing the duty cycle by decreasing t_1 (see Fig. 1(a)) narrows the mass window of the filter by increasing the average DC potential between the rods. The mass center of the window is shifted by changing the frequency of the applied waveform. The theory of this operating mode has been well documented [4,6].

Our manipulation of the applied waveforms to create a mix of a z-axis trapping/ejection field with a radial trapping field is new. Its effect on the behavior of the ions has not been discussed in the literature. An example of a trapping waveform is depicted in Fig. 1(b). The waveform on one rod set is created by shifting the duty cycle away from the normal 50% value; however, the waveform applied to the second rod set is created by shifting the phase instead of inverting the waveform. This manipulation creates a period where all four rods have the same potential. The potential difference between the rods and the end cap electrode create the axial trapping field during this period. However, when all four rods have the same potential, the quadrupole field is turned off for that part of the waveform period. There is no net electric field between the rods during this interval. This can be seen by
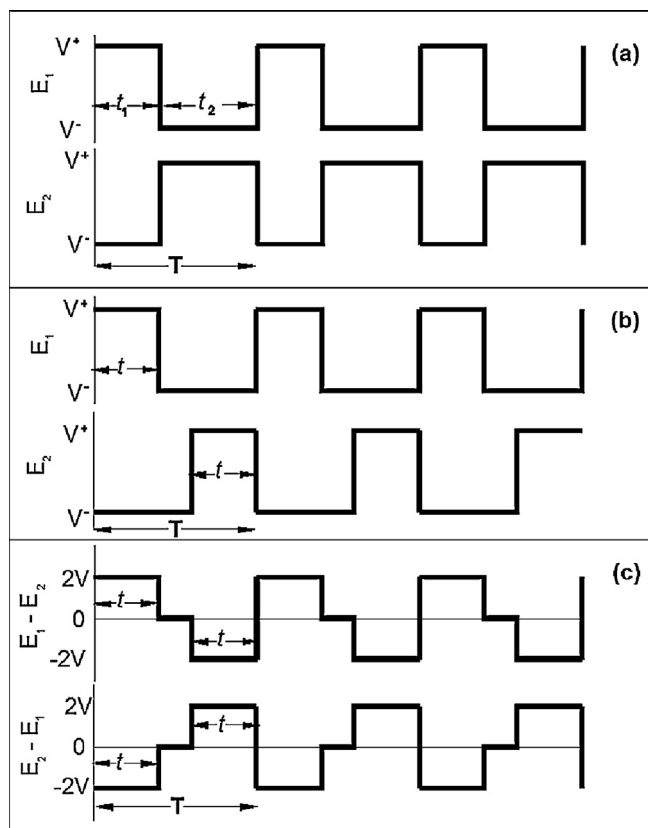
Fig. 1. (a) Duty cycle manipulation to permit the operation of a digital quadrupole as a mass filter. (b) Duty cycle manipulation that permits axial trapping while maintain radial trapping. (c) The potential difference between the rod sets when the axial trapping waveform is applied. It shows that the radial trapping field is zero when the axial trapping conditions are applied.
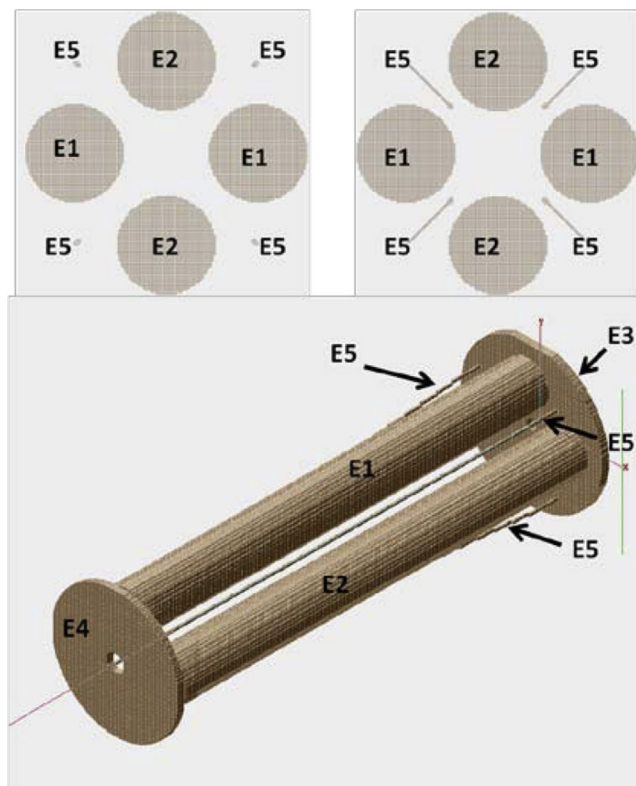

Fig. 2. Depiction of the electrode system used to simulate the ion trajectories during duty cycle based manipulation of the applied waveforms. The inset at the top left depicts the cross section of the quadrupole near the entrance end cap electrode. The right inset depicts the cross section near the exit end cap electrode.

subtracting the waveforms from each other ($E_1 - E_2$ and $E_2 - E_1$) in Fig. 1(c).

Turning off the radial field for a portion of the waveform cycle affects the motion of the radially trapped ions. Their secular frequencies change because the radial force is not applied for as long as it is when the duty cycle is 50%. Consequently, the minimum trapping frequency decreases for a given change in the duty cycle. How these quantities change with duty cycle needs to be understood in order to perform ion isolation while in this mode of operation. In this work, the change in the minimum trapping frequency as a function of duty cycle was determined by ion trajectory modeling and matrix methods applied to investigate the stability of the solutions of the Hill equation [6]. This provides a method for determining the low mass cut off of the quadrupole. We then used the same matrix methods to devise a new waveform manipulation that permits ions above and below the mass of interest to be selectively ejected from the linear quadrupole. This isolation process was verified by simulation.

2. SIMION modeling

The software used in ion trajectory modeling was SIMION 8.0 (Scientific Instrument Services, Inc., Ringoes, NJ). The linear quadrupole ion trap is modeled as shown in Fig. 2. The scaling used in the SIMION simulation was 0.55 grid units per mm (gu/mm). The simulated quadrupole rod length was 264 cm with a rod radius of 1.375 cm, and a radial distance, $r_0 = 1.21$ cm from the z-axis to the nearest surface of each rod. The end cap electrodes were circular 4.07 cm diameter disks with 0.495 cm diameter circular holes.

Four additional 1.1 mm thick slanted wire electrodes were placed between the quadrupole rods along the asymptotes. The tilt of the slanted wire electrodes is depicted in cross sectional insets in Fig. 2. The cross section near the entrance end cap electrode is depicted on the left and the cross section near the exit end cap electrode on the right. The distance between the slanted wire electrodes and the central axis of the quadrupole range from 18.67 to 35.78 mm. The five electrode sets include two opposite sets of rods (E1 and E2), entrance end cap (E3), exit end cap (E4) and the slanted wire electrodes (E5). The ions examined in the simulations discussed were positive and have mass-to-charge ratios that range from 10,000 to 1,000,000. The AC voltages for ion trapping applied to E1 and E2 were 500 V and −500 V for all simulations. An axial DC voltage can be added to the AC trapping potentials to adjust the kinetic energy of the ejected ions when needed. The slanted wire voltages used was −250 V. A nitrogen buffer gas was used at 7.5 mTorr for all simulations.

The user program to digitally operate the quadrupole was created by modifying the standard ion trap demo program to produce rectangular waveforms with controllable frequency, duty cycle and phase. A hard sphere, elastic, ion-neutral collision model was part of the demo program. It was used to simulate the effect of the buffer gas on the large ions.

3. Matrix method solution to the Hill equation

The process of using matrix methods to calculate independent solutions to the Hill equation has been described in detail [7]. The methods described in reference [7] have been more recently applied to determine the stability diagram that results from a pulsed bipolar waveform [6]. This was accomplished by dividing the full period of the function into finite elements where the voltage is constant in each element. For each element, the solution of the

Hill equation was calculated exactly. The solution over the entire period T was then calculated consecutively to provide the stability diagram [6]. Our duty cycle based axial trapping/ejection waveform is a special case of this stability diagram where there is no DC potential between the rods and the value of the Mathieu parameter a is zero.

Although Konenkov et al. [6] meticulously calculated the stability diagram for pulsed dipolar waveforms based on the procedure developed in reference [7], they did not discuss the effect of these waveforms on the ions. Moreover, their presented discussion does not enlighten the reader to the possibility of using these waveforms to axially trap and eject ions on demand in well collimated ion packets with well defined kinetic energy. Furthermore, there is no discussion of the change in the minimum trapping frequency, ion secular frequency or the boundary conditions with the change in duty cycle. While this information is implicit in the matrix calculations and can be extracted from them, it cannot be directly gleaned from the depiction of the stability diagram for a single duty cycle. Because this innovation is key to obtaining well resolved time-of-flight mass analysis in the ultra high mass range ($m/z > 20,000$) and understanding its effect on the motion of the ions is crucial, we feel justified in repeating and presenting the matrix calculations for the special case where the Mathieu parameter a is set to zero so that the effect of changing the duty cycle on the motion of the ions could be discussed and presented in the literature for the first time.

In order to define the radial stability of the ions by matrix methods, the transfer matrix M must be determined for one period of the waveform. It is the product of the matrices of all the constant voltage intervals over the cycle. From Fig. 1(c), there are three values of the voltage difference between the rod sets for three intervals during the cycle. In the notation of reference [6], the transfer matrix for stable solutions to the Hill equation is given by:

$$M = V(f_1, \tau) \times V(0, \pi - 2\tau) \times V(f_2, \tau)$$

$$M = \begin{pmatrix} \cos(\tau\sqrt{f}) & \frac{1}{\sqrt{f}}\sin(\tau\sqrt{f}) \\ -\sqrt{f}\sin(\tau\sqrt{f}) & \cos(\tau\sqrt{f}) \end{pmatrix} \times \begin{pmatrix} 1 & \pi - 2\tau \\ 0 & 1 \end{pmatrix} \times \begin{pmatrix} \cosh(\tau\sqrt{f}) & \frac{1}{\sqrt{f}}\sinh(\tau\sqrt{f}) \\ \sqrt{f}\sinh(\tau\sqrt{f}) & \cosh(\tau\sqrt{f}) \end{pmatrix} \quad (1)$$

Here ($\tau = \pi^* t/T$) and 2τ defines the interval that the quadrupolar field is present during the waveform cycle. $f_1 = f_2 = f$ and $f = 8ezV/mr_0^2\Omega^2$ where ez is the ion charge, V is the rf voltage zero to peak, m is the ion mass, r_0 is the quadrupole radius and Ω is the radial frequency. The trapping frequency F is related to the radial frequency by the following: ($\Omega = 2\pi F$). The variable f is given by the Mathieu parameter q times a constant. The calculation of q does not change with waveform duty cycle; however the value of q at the boundary does change because the definition of the boundary conditions change.

The trace of the transfer matrix supplies the criterion for stability as follows:

$$Tr(M) = |m_{11} + m_{22}| \leq 2$$

$$m_{11} + m_{22} = [2\cos(\tau\sqrt{f}) \times \cosh(\tau\sqrt{f})] + (\pi - 2\tau)(\sqrt{f}\sinh(\tau\sqrt{f}) \times \cos(\tau\sqrt{f}) - \sqrt{f}\sin(\tau\sqrt{f}) \times \cosh(\tau\sqrt{f})] \quad (2)$$

4. Results

The minimum value of the trapping frequency F was determined iteratively by finding the minimum value of Ω^2 that provided stable ions. The minimum trapping frequency as a function of the quadrupole field fraction 2τ was determined for singly charged bovine serum albumin ($m/z = 66,398$) first by simulation of our trapping system. The quadrupole field interval is the fraction of the waveform cycle that yields radial trapping of the ions. Our configuration uses slanted wire electrodes between the rods to create a small electric field along the z-axis of the quadrupole. This
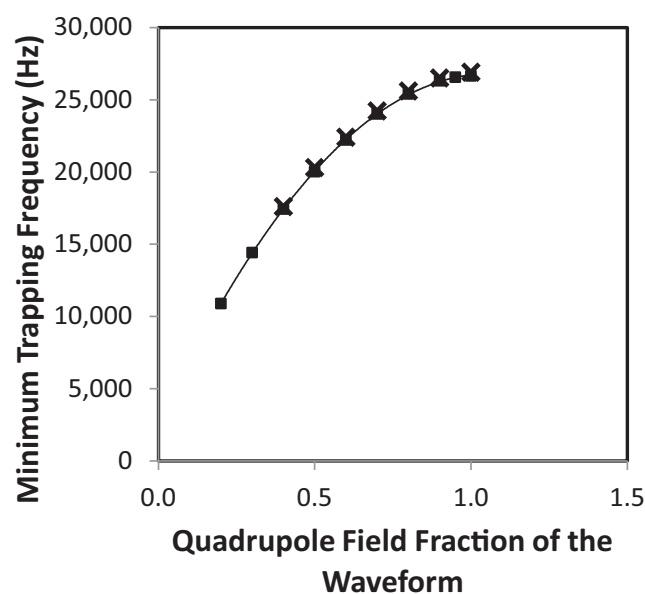

Fig. 3. The minimum trapping frequency for singly charged bovine serum albumin $m/z = 66,398$ as a function of fraction of the applied waveform that yields radial trapping (with a quadrupole field). The rest of the waveform fraction is used to provide axial trapping of the ions in the linear trap and turns off the quadrupole field. Turning off the quadrupole field changes the stability conditions and reduces the minimum trapping frequency. The black crosses are the result of ion trajectory simulation. The solid black square dots are the result of exact matrix based calculation. The solid line is a polynomial fit of the calculated data.

pushes the ions toward the exit end cap electrodes. The ions collect where the z-axis field and the duty cycle induced axial trapping field balance. Bunching the ions near the exit with axial fields was predicted to have a negligible effect on radial stability. The agreement between the simulations and the matrix calculations can be used to validate that prediction. The results of the simulation are depicted by the black exes at $2\tau = 0.4, 0.5, 0.6, 0.7, 0.8, 0.9$ and 1.0 in Fig. 3. $\tau = 1.0$ corresponds to a 50% duty cycle where there is no axial trapping field. As the interval of application of the quadrupole field decreases, the minimum trapping frequency decreases in a nonlinear fashion. The solid black square dots in Fig. 3 depict the minimum trapping frequency calculated by matrix methods. The calculation maps the simulation within 1%. The calculation of the matrix elements is exact when applied to rectangular waveforms. The difference between the simulation and the calculation is due to error that is inherent in ion trajectory simulations. The effect of the axial field induced by the wire electrodes on the ion stability is negligible.

5. Discussion

The change in the minimum trapping frequency with duty cycle results from the change in the boundary condition caused by
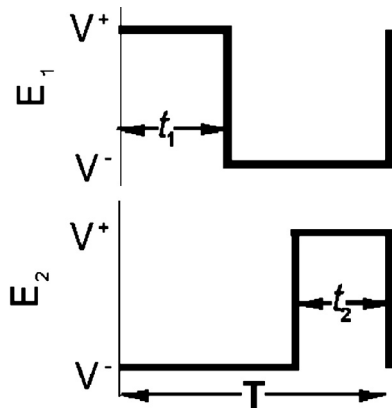
Fig. 4. Duty cycle based waveform manipulation that permits precise ion isolation while permitting axial trapping.

Fig. 5. Plot of m/z as a function of quadrupole waveform frequency used to define the stability of ions for a 35/40/25 quadrupole waveform. The black dots represent simulated results. The black trend lines depict least squares fits of the simulated data. The shaded region depicts the matrix derived region of stability.

turning off the radial quadrupole field for a varied fraction of the waveform. This can be seen in Eq. (2). When the duty cycle is 50% the quadrupole field is not turned off during the waveform cycle and $\tau = 0.5$ making the middle term in the trace of the transfer matrix (Eq. (2)) zero. When the $1-2\tau$ term becomes non-zero with a change in duty cycle then the boundary condition changes. The boundary condition is also defined by the following:

$$2\cos(\pi\beta) = m_{11} + m_{22} \tag{3}$$

The integer values of β define the boundaries of the stability diagram. The relationship between β and the ion secular frequency ω_{sec} is still valid when the duty cycle is changed.

$$\omega_{sec} = \frac{\beta\Omega}{2} = \frac{\Omega}{2\pi}\arccos(m_{11} + m_{22}) \tag{4}$$

Consequently, the secular frequency change with duty cycle is exactly calculable and the ion motion is completely definable when the duty cycle based waveform manipulations are applied. The conditions for stability are definable at any duty cycle. Therefore, duty cycle manipulated waveforms can be used to eject unwanted ions for selective mass isolation.

So far, we have shown that the low mass cut off trapping frequency (i.e., the minimum trapping frequency) can be calculated for our axial trapping and ejection waveforms. Therefore, the ions with masses below the ion of interest can be filtered out. A methodology for isolation of ions of greater mass from the ions of interest using bipolar pulsed waveforms with the special case of $a = 0$ would be beneficial. Konenkov et al.'s work [6] shows how to perform that isolation by changing the Mathieu parameter, a. It does not reveal how to perform ion isolation while a remains at zero. Requiring a to change to perform ion isolation complicates the instrumentation. It requires control of the DC power supplies that operate the high voltage pulsers to produce the waveforms. Those DC levels have to be changed on the fly to perform the isolation. Moreover, it requires four separate power supplies (two for each rod set). Whereas if the ion isolation is performed with the Mathieu parameter a always set to zero, the DC potentials that define the high voltage waveforms can remain constant throughout the experiment and only two DC power supplies are needed to operate both sets of pulsers. Consequently, developing the ability to perform ion isolation with $a = 0$ is a worthwhile endeavor.

Ions above the mass of interest can be ejected while using duty cycle based axial trapping by combining the waveforms in Fig. 1(a) and (b). The applied waveform combination strategy for ion isolation is shown in Fig. 4. In this case, the duration of the waveform high applied to each electrode set is different, $t_1 \neq t_2$, while there is still a period that both rod sets have the same axial trapping potential (see Fig. 4). When $t_1 \neq t_2$, a DC potential exists between
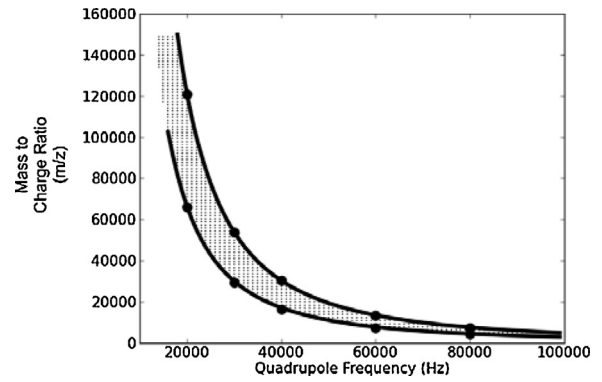
the rods when the radial potential is applied that narrows the mass window. The frequency of this waveform can be scanned or jumped to precisely eject the masses. Matrix calculations for this particular type of waveform do not currently exist in the literature. The stability conditions for this waveform are also precisely calculable using the same matrix methods applied by Konenkov et al. [6] and originally developed by Pipes [7]. Here the transmission matrix is given by:

$$M = V(f_1, \tau_1) \times V(0, \pi - \tau_1 - \tau_2) \times V(f_2, \tau_2)$$

where $\tau_n = \pi(t_n/T)$ and $\tau_1 + \tau_2$ defines the interval that the quadrupolar field is present during the waveform cycle and $\pi - (\tau_1 + \tau_2)$ defines the duration of the axial trapping and ejection field. $f_1 = f_2 = f$ and $f = 8ezV/mr_0^2\Omega^2$. Fig. 5 illustrates a version of the stability diagram that is more useful for ion isolation than that normally used for sinusoidal ion traps. It plots ion stability as a function of m/z and quadrupole frequency (Hz) instead of the Mathieu parameters a and q. Plotting the stability diagram as a function of a and q is not very useful because both of these parameters are dependent on the trapping frequency. Therefore, navigating an a versus q stability diagram by changing the trapping frequency is not intuitively obvious. In the illustrated example in Fig. 5, for 35% of the waveform cycle all four rods have the same potential and thereby permits axial trapping. The quadrupolar field then is applied for 65% of the cycle. τ_1 was set to 0.40π and τ_2 was set to 0.25π. This waveform is annotated as a 35/40/25 duty cycle based waveform. The first number in the annotation defines the duration of the axial trapping field while the second and third define the duty cycle of the quadrupole portion of the waveform. The three numbers are required to sum to 100. The shaded area of the graph in Fig. 5 represents the region of stability as a function of ion mass-to-charge ratio and trapping frequency. Therefore, for a given mass, the range of stable quadrupole frequencies is defined by the shaded region for that mass projected on the x-axis. To isolate that given mass, the frequency of the waveform would simply have to be jumped from one extreme of the stable frequency range to the other.

This calculation was validated by simulation. For ions of selected values of m/z, the maximum and minimum stable frequencies were determined. These values are depicted in Fig. 5 as solid dots. The maxima and minima of the stability region were then defined by least squares using an exponential function to fit the points. The least squares trend lines are depicted as solid black lines. These simulation derived boundaries closely map the edges of the matrix derived stability region and are therefore in good agreement.

The resolution of the isolation depends on the precision and the resolution of the applied waveforms in the same way that was observed by Ding et al. when they performed mass isolation in a

3D digital ion trap [8]. They showed that their ability to isolate ions was defined by the resolution of the forward and backward scans. There they revealed an ion isolation resolution exceeding 3500. Because the electrode configuration in our linear quadrupole and Ding et al.'s 3D ion trap are both unstretched, we expect a similar performance. The exhibited 3500 mass resolving power $(m/\Delta m)$ would permit a protein such as bovine serum albumin (66 kDa) to be isolated within a 19 u mass window. Consequently, mass isolation by this method should provide sufficient resolution to isolate intact singly charged proteins.

The thickness of the stability region changes with the difference between τ_1 and τ_2. When $\tau_1 = \tau_2$, the thickness of the band of stability (the shaded region) is maximum (see Fig. 5). Theoretically, any mass above the minimum stable mass is stable when $\tau_1 = \tau_2$ just as it is for an ion trap or guide. Naturally, the pseudo-potential well depth still decreases with increasing m/z so the trapping mass range is limited in the same manner as sinusoidal ion traps and guides. The greater the difference between τ_1 and τ_2, the more narrow the band of stability or the range of stable frequencies for a given mass.

6. Conclusion

Duty cycle manipulated waveforms have been shown to be capable of ion isolation while providing axial trapping by both simulation and matrix calculation. The matrix calculations exactly define the stability region of the ion mass to charge ratio as a function of quadrupole waveform frequency. Methodology for frequency-based ion isolation while maintaining duty cycle based axial trapping was presented. The changes in the boundary conditions and ion motion with the applied duty cycle manipulations were discussed.

References

[1] J. Lee, M.A. Marino, H. Koizumi, P.T.A. Reilly, Simulation of duty cycle-based trapping and ejection of massive ions using linear digital quadrupoles: the enabling technology for high resolution time-of-flight mass spectrometry in the ultra high mass range, International Journal of Mass Spectrometry 304 (2011) 36–40.

[2] J. Lee, H. Chen, T. Liu, C.E. Berkman, P.T.A. Reilly, High resolution time-of-flight mass analysis of the entire range of intact singly-charged proteins, Analytical Chemistry 83 (2011) 9406–9412.

[3] X. Wang, H. Chen, J. Lee, P.T.A. Reilly, Increasing the trapping mass range to m/z = 109—a major step toward high resolution mass analysis of intact RNA, DNA and viruses, International Journal of Mass Spectrometry 328–329 (2012) 28–35.

[4] J.A. Richards, R.M. Huey, J. Hiller, A new operating mode for the quadrupole mass filter, International Journal of Mass Spectrometry and Ion Processes 12 (1973) 317–339.

[5] F.L. Brancia, B. McCullough, A. Entwistle, J.G. Grossmann, L. Ding, Digital asymmetric waveform isolation (DAWI) in a digital linear ion trap, Journal of the American Society for Mass Spectrometry 21 (2010) 1530–1533.

[6] N.V. Konenkov, M. Sudakov, D.J. Douglas, Matrix methods for the calculation of stability diagrams in quadrupole mass spectrometry, Journal of the American Society for Mass Spectrometry 13 (2002) 597–613.

[7] L.A. Pipes, Matrix solution of equations of the Mathieu–Hill Type, Journal of Applied Physics 24 (1953) 902–910.

[8] L. Ding, M. Sudakov, F.L. Brancia, R. Giles, S. Kumashiro, A digital ion trap mass spectrometer coupled with atmospheric pressure ion sources, Journal of Mass Spectrometry 39 (2004) 471–484.